Fermi National Accelerator Laboratory

DD

FERMILAB-FN-619

SC 9428

How to Optimize the CMS Hadron Calorimetry by Assigning Weights to Layers

A. Beretvas, D. Green, J. Marraffino and W. Wu

Fermi National Accelerator Laboratory
P.O. Box 500, Batavia, Illinois 60510

CERN LIBRARIES, GENEVA

P00024346

May 1994

Operated by Universities Research Association Inc. under Contract No. DE-AC02-76CHO3000 with the United States Department of Energy

Disclaimer

This report was prepared as an account of work sponsored by an agency of the United States Government. Neither the United States Government nor any agency thereof, nor any of their employees, makes any warranty, express or implied, or assumes any legal liability or responsibility for the accuracy, completeness, or usefulness of any information, apparatus, product, or process disclosed, or represents that its use would not infringe privately owned rights. Reference herein to any specific commercial product, process, or service by trade name, trademark, manufacturer, or otherwise, does not necessarily constitute or imply its endorsement, recommendation, or favoring by the United States Government or any agency thereof. The views and opinions of authors expressed herein do not necessarily state or reflect those of the United States Government or any agency thereof.

How to optimize the CMS Hadron Calorimetry by assigning weights to layers

A. Beretvas, D. Green, J. Marraffino, and W. Wu

Fermi National Accelerator Laboratory, Batavia, Illinois, 60510.

Version 1.0 May 10, 1994.

1 Introduction

The CMS Letter of Intent describes the Calorimetry for the proposed detector [1]. An important task for a high energy calorimeter is the measurement of dijet masses [2]. Typically depths in the range of 9-11 absorption lengths (λ) were specified by the SDC and GEM detectors. The CMS detector achieves this depth of absorption lengths by adding a "tail catcher" outside of the magnet coil, introducing the problem of inert material within the active volume of the calorimeter. We have previously looked at a similar problem caused by a thin (10.7 cm of Al) superconducting coil being placed in front of the SDC EM calorimeter [3]. We have also looked at the effect of energy leakage due to the finite length of the calorimeter and found that effect can be compensated by assigning higher weights to the rear layers of the calorimeter[4]. The inert material can also potentially induce missing transverse energy signals which are large with respect to real physics signatures. In this paper we try to find the optimal energy resolution for the CMS hadron calorimeter by assigning variable weights to the layers in front of the coil and in the "tail catcher".

2 Baseline CMS Hadron Calorimeter

The hadron calorimeter (preferred option) uses copper as the absorber; the active element is plastic scintillator. In our study we consider the nominal depth of the hadron calorimeter before the magnet coil to be 5.9 λ. The coil is treated as dead material with an absorption length of 1.4 λ. Then outside the field we consider a "tail catcher" of 2.1 λ.

3 Experimental Hadron Data

We use hadron data from the LAB E experiment [5]. That hadron calorimeter was 19.2 λ deep and was read out at sampling intervals of 0.7 λ starting at 0.3 λ. To simulate the CMS hadron calorimeter we consider the first 9 layers as being inside the copper absorber, the next two layers are inside the coil and are turned off and the next three layers are in the "tail catcher". We have used MINUIT and taken a weight of 1 for the first 6 layers, a variable weight for the next three layers, a weight of 0 for the next two layers and finally a variable weight for the last 3 layers. Note that test beam data with a steel calorimeter is used. The CMS coil is aluminum, so that the present analysis overestimates the effect of the inert coil material. The data set used here consists of pions incident at momentum of 25, 50, 200 and 450 GeV. The longitudinal shower profiles are illustrated in Figure 1.

4 Weights found by MINUIT

We will show results for 4 cases. The first is for an infinite calorimeter (actually 19.2 λ corresponding to 27 layers), the second is for a truncated calorimeter of length 9.4 λ corresponding to 14 layers, the third is for a calorimeter of length 9.4 λ but with layers 10 and 11 turned off, and finally a

calorimeter of 14 layers (9.4 λ) with layers 10 and 11 turned off and optimized variable weights assigned to the three layers before and after the coil. The optimum weights were defined to be those which minimize the RMS of energy variation with respect to the energy measured in a calorimeter of depth 19.2 λ. The results are found in Table 1. The weight factors at minimum RMS are given in Table 2.

5 Results

Clearly the best resolution is obtained by the infinite calorimeter. A calorimeter of 9.4 λ causes the resolution to be degraded by an amount which increases with energy as expected. With inert layers the resolution is futher degraded. The resolution at all energies is clearly improved by weighting of the 6 independent longitudinal segments.

Figure 2 shows the 4 cases we have considered for 200 GeV incident hadrons. The infinite calorimeter as expected is best able to reconstruct the beam energy without tails and also yields the smallest RMS. The 9.4 λ calorimeter reconstructs the energy low by 1.6 %, and has an RMS that is increased by 14.3 %. If layers 10 and 11 are made inert the energy is reconstructed low by 7.5 % and the RMS is increased by 73.7 % relative to the infinite calorimeter. By weighting, both the mean of the energy and the energy sigma are improved. The energy is reconstructed low by 1.5 % and the RMS is increased by 46.8 % relative to the infinite case.

6 Two and Four Parameter fits

Essentially the same results are obtained by using far fewer parameters. The results of a four parameter fit are given in Table 3. The four parameters are the weights for one layer in front of

the coil and 3 layers behind the coil (note that layers 7 and 8 have unit weight). In fact, almost the same results can be obtained from a two parameter fit (see Table 4). The two parameters are the weight for the one layer upstream of the coil and identical weights for the three layers after the coil. Almost identical results have been obtained [6] using the "Hanging File" data [7] and a different minimization procedure.

7 Location of the dead region

In addition to the standard CMS configuration which has the coil in the region of layers 10 and 11, we have investigated a "long" version in which the dead region has been moved back by 0.7 λ, and a "short" version in which the dead region has been moved forward by 0.7 λ. As expected the long version gives the best resolution and the short version yields the worst resolution. The quantitative results are presented in Table 5 and 6. Again comparable results are obtained by using a two parameter fit (see Table 7). Note that the simple fit might easily be realized with 3 independent calorimeter readouts. For a beam energy of 200 GeV we show in Figure 3 the results for a weighted fit for the long, standard and short configurations.

8 Measuring the total energy

Figures 4 - 7 show the percentage of the total energy, defined as the measured energy in a 19.2λ depth, that is measured by the truncated hadron calorimeter. The top plot in all four figures is for the standard CMS configuration (a 5.9 λ deep calorimeter interrupted by an inert 1.4 λ deep coil followed by a 2.1 λ tail catcher) with uniform weighting of one. The bottom plot is the same calorimeter where we have given a weight of 1.5 to the 3 layers in front of the coil and a weight of

2 to the 3 layers in the tail catcher. In all cases we see that for the bottom plot the mean is higher and the RMS is smaller. The largest improvement, as expected, is at 450 GeV where the RMS is reduced by almost a factor of two.

9 Early and Late Showers

We have divided the hadron calorimeter into two sections (HAC1,HAC2). The first section contains 5 layers (3.1λ) and the second contains 4 layers (2.8λ). Figure 8 shows the ratio of hadronic energy in the first section to that in the second section. We see that as the incident energy increases the ratio of HAC1 to HAC2 decreases indicating that the shower maximum occurs later. The results for the energy resolution are given in Table 8. The table shows that for a 25 GeV incident pion if the ratio of HAC1 to HAC2 is less than 3.95 the energy resolution is 17.14%, but if the ratio is greater than 3.95 then the resolution is 17.83%. Ongoing attempts to use this information to further improve the energy resolution are being made.

10 Missing E_T

It is important to see if the Missing E_T resolution of the detector is compromised by the design. We have developed a simplified detector simulation program called SSCSIM. This program was used in conjunction with the SDC calorimeter and has recently been modified to approximately correspond to the CMS detector.

We have calculated (see Figure 9) the QCD dijet cross section as a function of missing E_T ($\not{E}_T$). The Figure shows what this distribution would look like with a 6 λ and 9 λ deep unweighted calorimeter. Clearly at a fixed $\not{E}_T$ of about 500 GeV an unweighted 6 λ deep calorimeter increases

the cross section by a factor of about 30. We also show the magnitude of the missing E_T cross section for the production of gluinos of mass 300 GeV and 1000 GeV. In order to see these signals additional cuts need to be applied. In Figure 10 we show the $\not{E}_T$ response for QCD dijet events for both a standard unweighted CMS calorimeter and a weighted one. Almost a factor of 10 improvement in cross section is achieved by using a weighted response from the calorimeter. Further possible improvements are being studied.

References

[1] Letter of Intent by the CMS Collaboration for a General Purpose Detector at the LHC CERN/LHCC92-3 LHCC/I1, 1 October 1992.

[2] D. Green, A. Beretvas, K. Denisenko, N. Denisenko, J. Marraffino and W. Wu, "Depth Requirements in SSC Calorimeters" SDC-91-00016, Fermilab FN-570, August,1991.

[3] J. Marraffino, W. Wu, A. Beretvas, D. Green, K. Denisenko and A. Para, ""Massless Gaps" for Solenoid+Calorimeter" Fermilab-TM-1766, November 1991.

[4] A. Beretvas, D. Green, J. Marraffino, and W. Wu, "A Weighting Strategy for Compensating Leakage in the SDC Electromagnetic Calorimeter" Fermilab-FN-587, April 1992.

[5] W. K. Sakumoto *et al.*, "Calibration of the CCFR Target Calorimeter" Nucl. Instr. and Meth. **A294**, 179 (1990). We have used the Lab E data, private communications from W. K. Sakumoto.

[6] Dan Green,"Missing Energy Induced by Thin Hadron Calorimeter" Fermilab, April 1994.

[7] A. Beretvas *et al.*, "Beam Tests of Composite Calorimeter Configurations from Reconfigurable-Stack Calorimeter" Nucl. Instr. and Meth. **A329**, 50 (1993).

C1	Infinite calorimeter 19.2 λ			
C2	9.4 λ calorimeter			
C3	9.4 λ calorimeter and inert coil			
C4	same as C3 but with optimal weighting			
Energy(GeV)	C1	C2	C3	C4
25	16.87	16.95	18.63	17.87
50	12.24	12.62	14.44	13.45
200	6.11	6.40	7.53	7.11
450	4.13	4.50	5.56	5.13

Table 1: Energy resolution in % for the Hadron Calorimeter

Energy(GeV)	w7	w8	w9	w12	w13	w14
25	1.4	1.4	1.0	2.1	0.4	1.9
50	1.0	1.0	1.5	1.9	1.4	1.5
200	1.0	1.0	1.5	2.0	2.0	2.0
450	1.0	1.0	1.5	1.5	1.5	3.3

Table 2: Weight Factors for the Hadron Calorimeter

Energy(GeV)	w9	w12	w13	w14	dE/E (%)
25	1.53	2.0	2.0	0.8	17.94
50	1.52	1.8	1.8	2.2	13.57
200	1.51	2.0	2.0	2.0	7.13
450	1.50	2.0	2.3	2.0	5.09

Table 3: Weight Factors for minimizing the Energy resolution of the Hadron Calorimeter

Energy(GeV)	w9	w12=w13=w14	dE/E (%)
25	1.51	2.0	17.85
50	1.50	2.0	13.62
200	1.50	2.0	7.13
450	1.50	1.5	5.08

Table 4: Weight Factors for minimizing the Energy resolution of the Hadron Calorimeter

Energy(GeV)	configuration	C1	C2	C3	C4
25	long	16.87	17.31	18.00	17.57
	standard		16.95	18.63	17.87
	short		17.34	19.30	19.12
50	long	12.24	12.43	13.78	13.24
	standard		12.62	14.44	14.08
	short		12.82	15.71	14.84
200	long	6.11	6.33	7.13	6.80
	standard		6.40	7.53	7.29
	short		6.60	8.47	8.12
450	long	4.13	4.50	5.56	5.33
	standard		4.50	5.56	5.31
	short		4.63	6.41	5.63

Table 5: Energy resolution dE/E in % for a Hadron Calorimeter (RMS).

Energy(GeV)	configuration	w6	w7	w8	w9	w10	w11	w12	w13	w14	w15
25	long	1.	1.	0.7	1.5	1.5	0.	0.	1.5	1.5	1.1
	standard	1.	1.4	1.4	1.0	0.	0.	2.1	0.4	1.9	0.
	short	1.5	0.2	1.5	0.	0.	1.5	1.4	1.5	0.	0.
50	long	1.	1.	1.5	1.5	1.3	0.	0.	0.9	1.3	1.5
	standard	1.	1.1	0.9	1.3	0.	0.	1.4	1.5	1.6	0.
	short	0.7	1.5	1.4	0.	0.	1.1	1.3	1.5	0.	0.
200	long	1.	1.	1.5	1.5	1.5	0.	0.	1.5	1.5	1.5
	standard	1.	0.7	1.6	1.4	0.	0.	1.5	1.5	2.6	0.
	short	0.9	1.0	1.9	0.	0.	1.2	1.1	1.0	0.	0.
450	long	1.	1.	0.9	1.5	0.4	0.	0.	2.8	2.9	1.5
	standard	1.	0.7	1.5	1.5	0.	0.	1.5	1.5	1.5	0.
	short	1.2	1.2	1.2	0.	0.	1.3	1.4	1.5	0.	0.

Table 6: Weight Factors for minimizing the Energy resolution of the Hadron Calorimeter (RMS)

Energy(GeV)	configuration	C4 %
25	long	17.64
	standard	17.84
	short	18.24
50	long	13.16
	standard	13.64
	short	14.11
200	long	6.81
	standard	7.01
	short	7.67
450	long	4.86
	standard	5.11
	short	5.53

Table 7: Energy resolution dE/E in % for a Hadron Calorimeter (RMS). We have fitted using a weight of 1.5 for the 3 layers before the coil and a weight of 2 for the 3 layers after the coil.

Energy(GeV)	$\frac{\text{HAC1}}{\text{HAC2}}$	Early Shower %	Late Shower %
25	3.95	17.14	17.83
50	2.73	12.45	15.29
200	2.13	6.53	7.77
450	1.93	4.54	5.82

Table 8: Energy resolution dE/E in % for a Hadron Calorimeter (RMS). We have fitted using a weight of 1.5 for the 3 layers before the coil and a weight of 2 for the 3 layers after the coil.

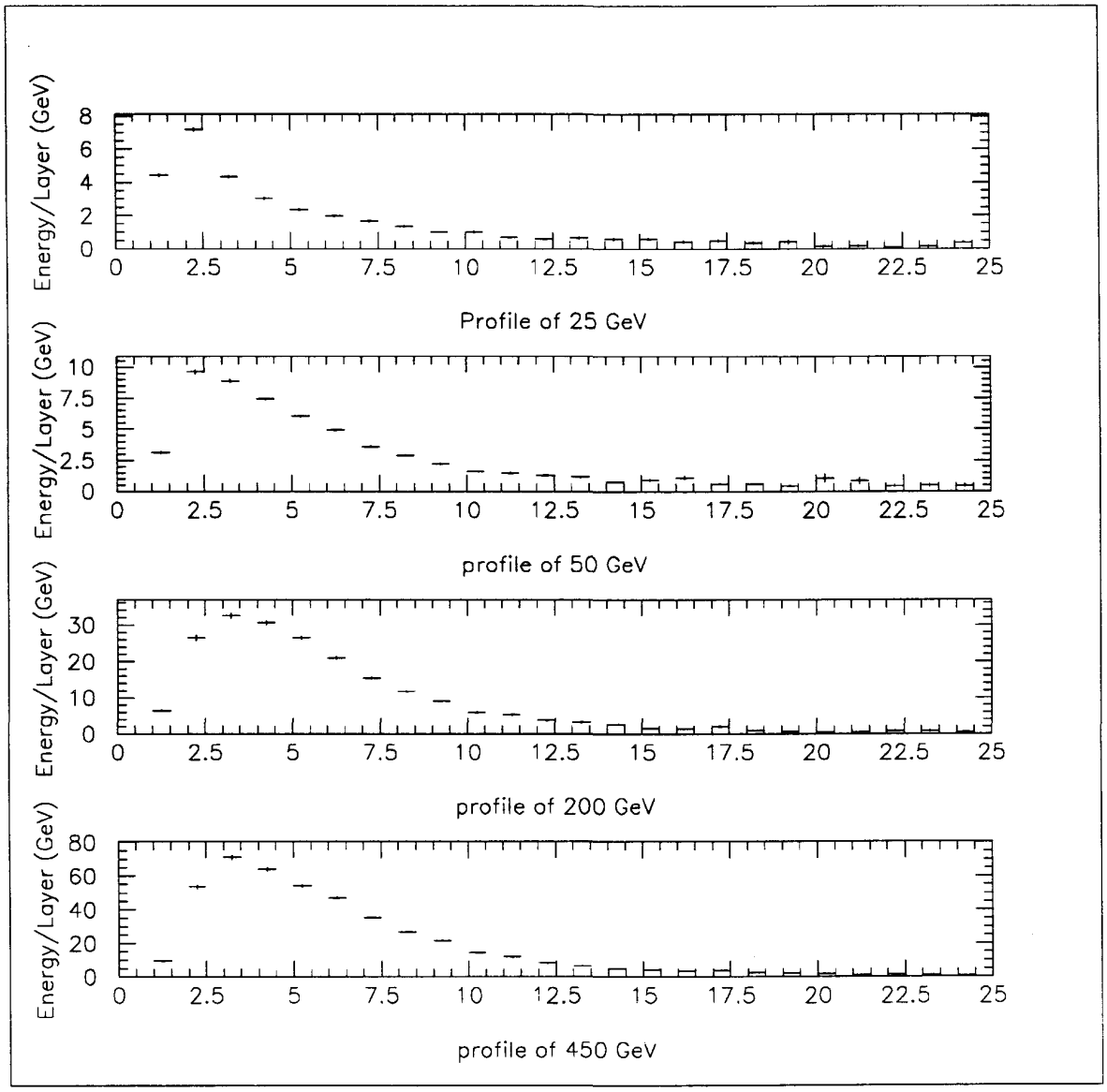

Figure 1: Longitudinal energy depth shower profile for pion beams of energy 25, 50, 200 and 450 GeV. The vertical scale shows the energy(GeV) deposited in each layer.

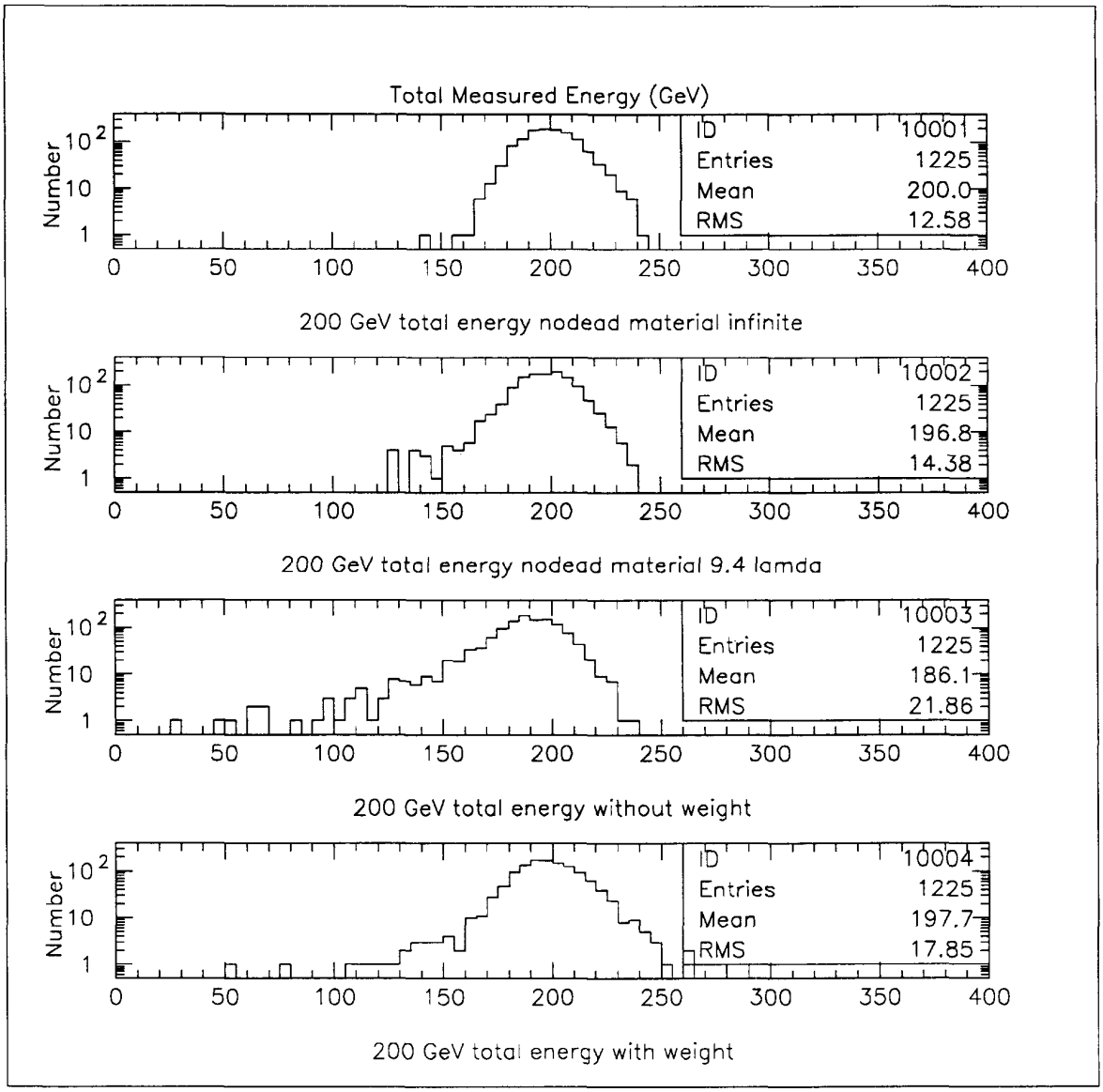

Figure 2: Reconstructed energy for 4 cases at 200 GeV. a) 19.2 λ calorimeter, b) 9.4 λ calorimeter, c) 9.4 λ with layers 10 and 11 missing, d) Same calorimeter as c) but with optimal weighting for 3 layers in front of the dead region and 3 layers behind the dead region.

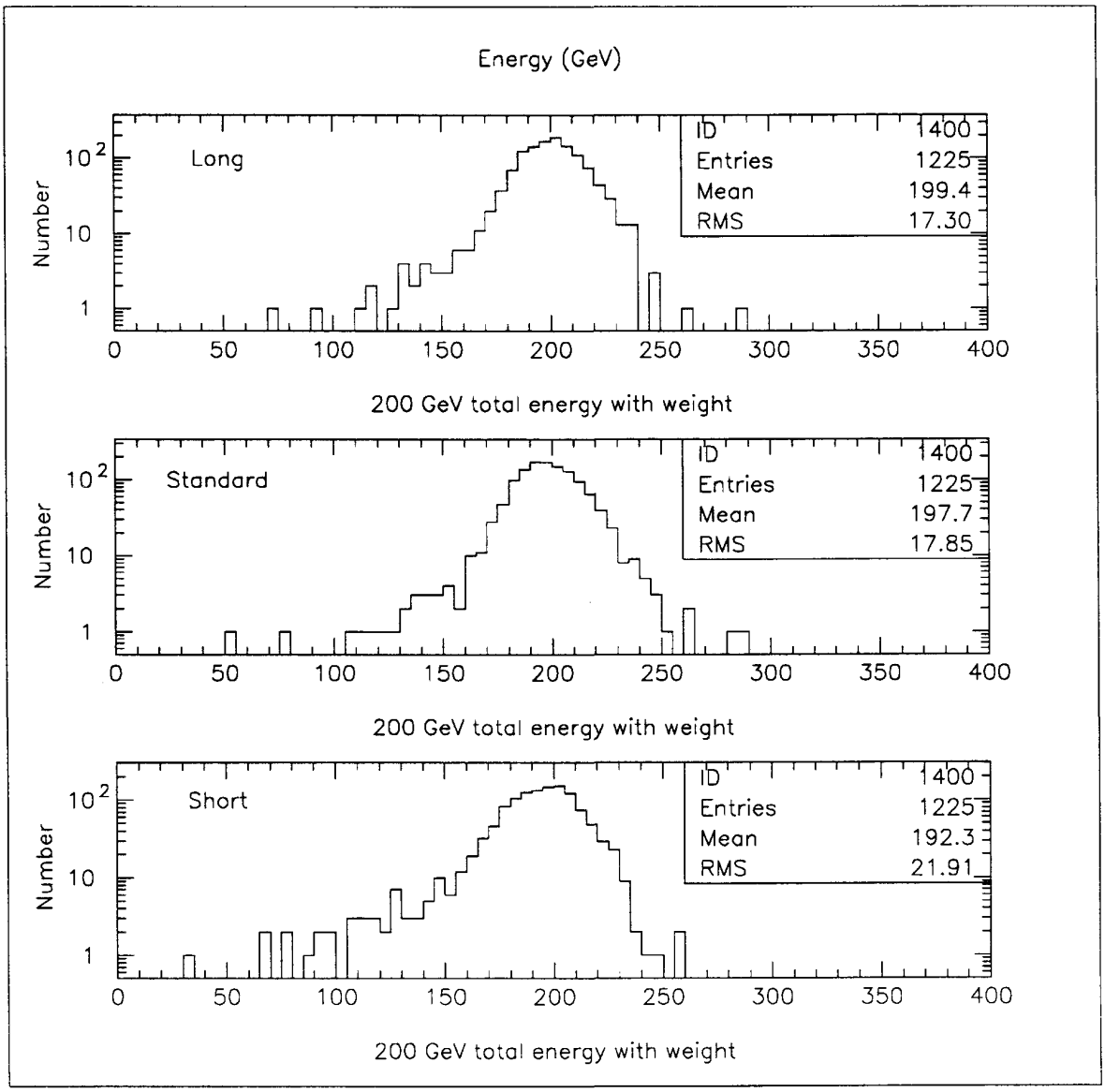

Figure 3: Reconstructed energy for a long, standard and short calorimeter at a beam energy of 200 GeV

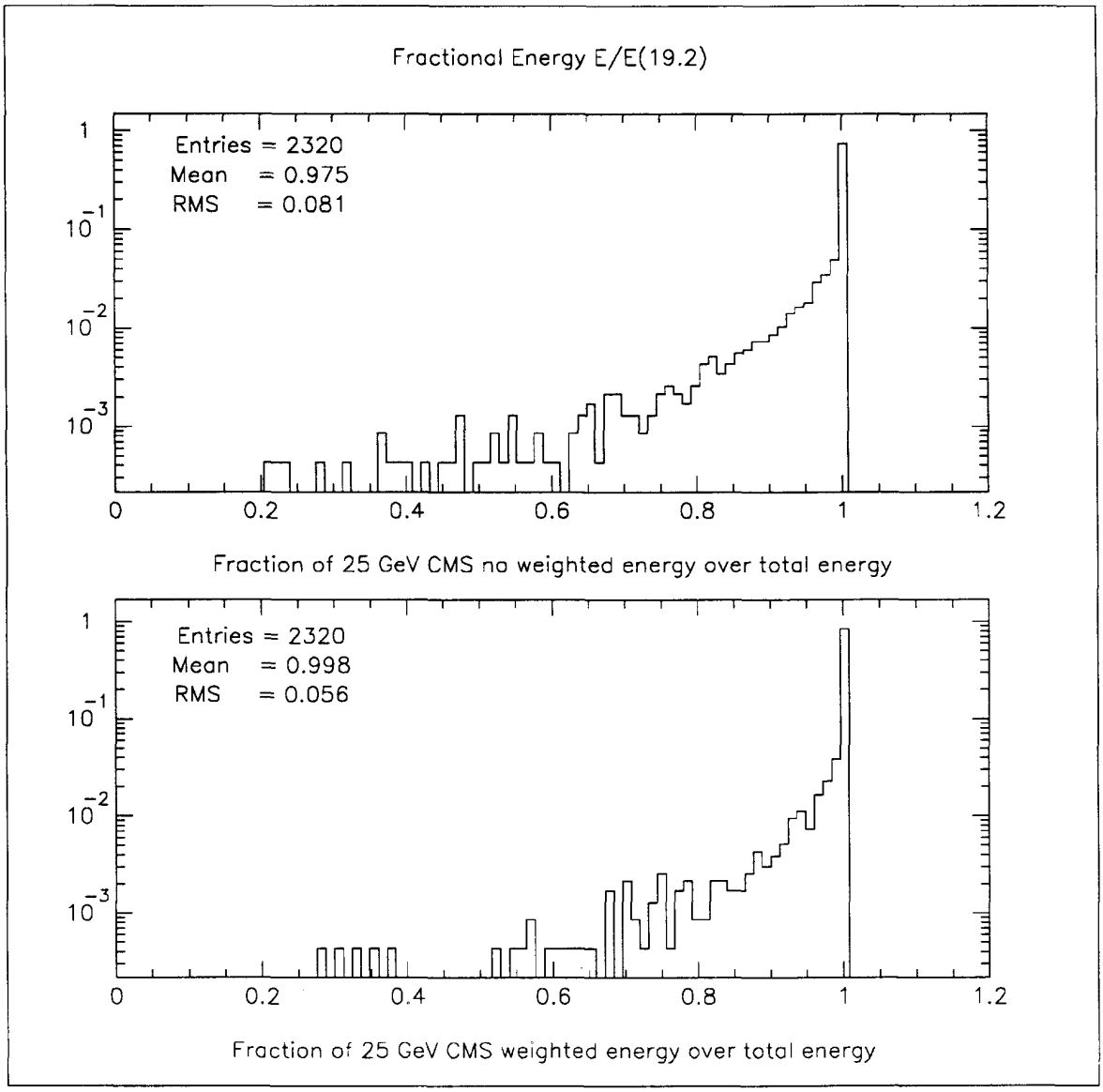

Figure 4: a) Fraction of events as a function of the fraction of the total energy for the Standard CMS calorimeter at a beam energy of 25 GeV. b) same as above, but using a calorimeter with weighting.

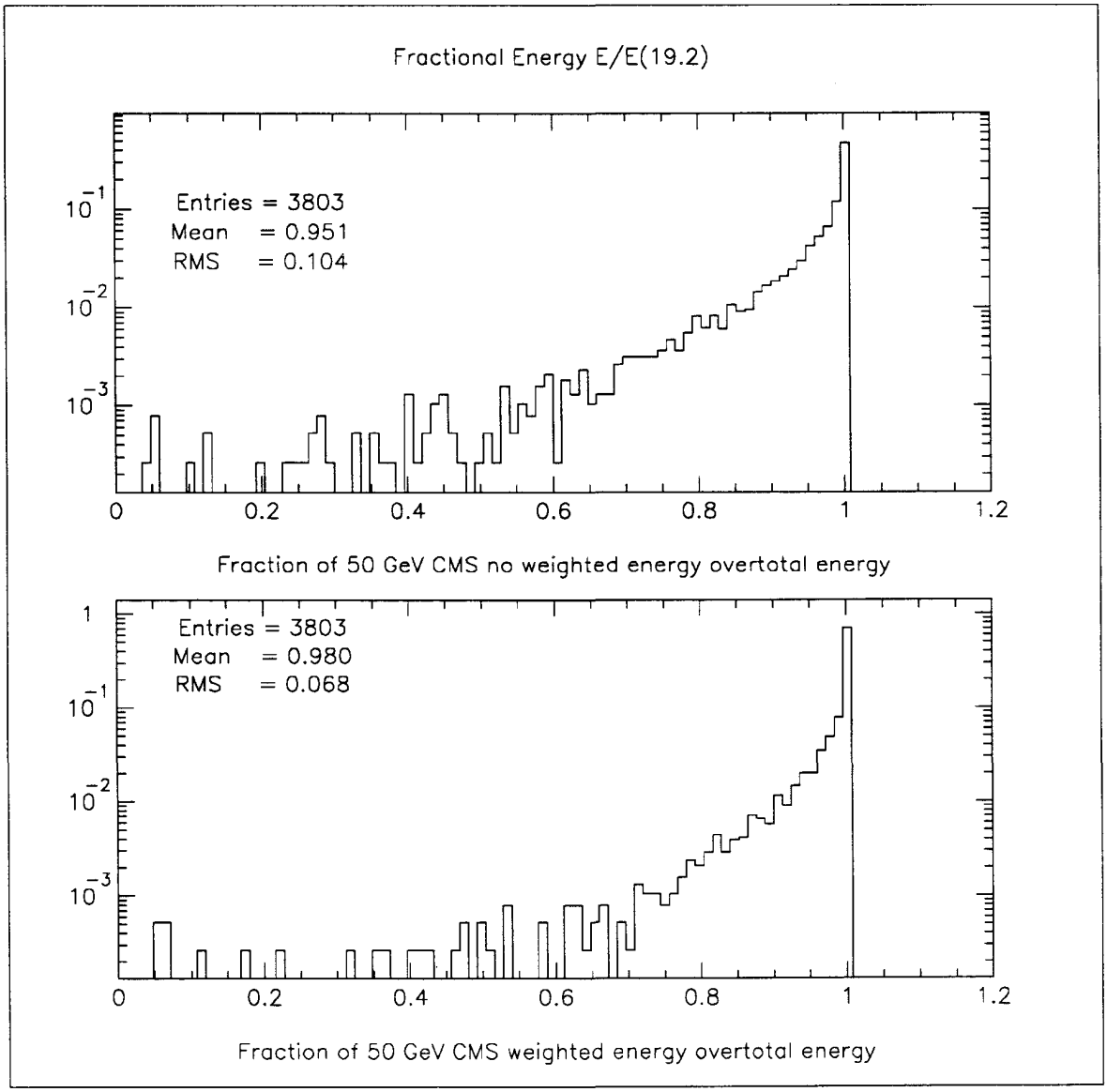

Figure 5: a) Fraction of events as a function of the fraction of the total energy for the Standard CMS calorimeter at a beam energy of 50 GeV. b) same as above, but using a calorimeter with weighting.

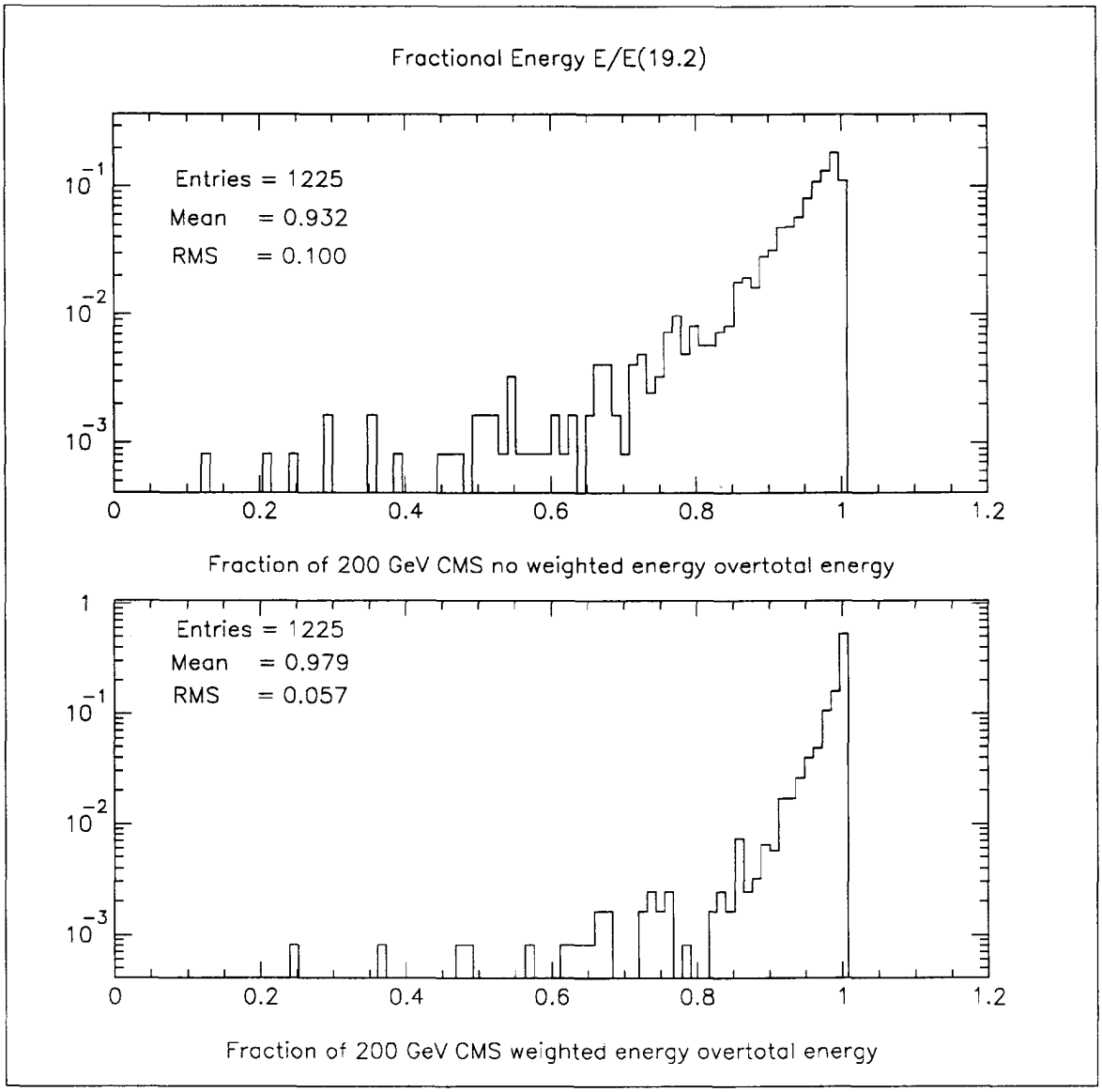

Figure 6: a) Fraction of events as a function of the fraction of the total energy for the Standard CMS calorimeter at a beam energy of 200 GeV. b) same as above, but using a calorimeter with weighting.

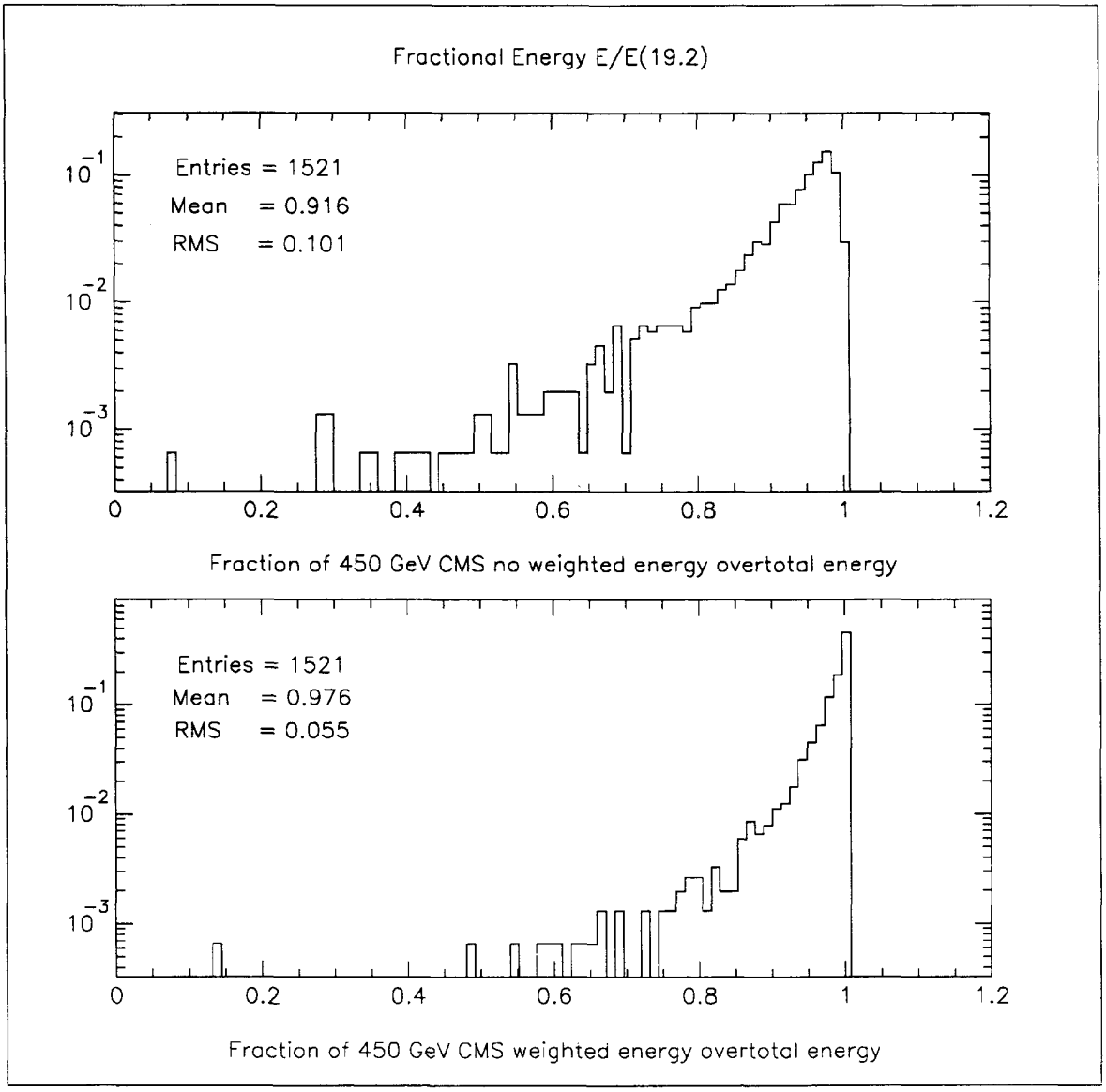

Figure 7: a) Fraction of events as a function of the fraction of the total energy for the Standard CMS calorimeter at a beam energy of 450 GeV. b) same as above, but using a calorimeter with weighting.

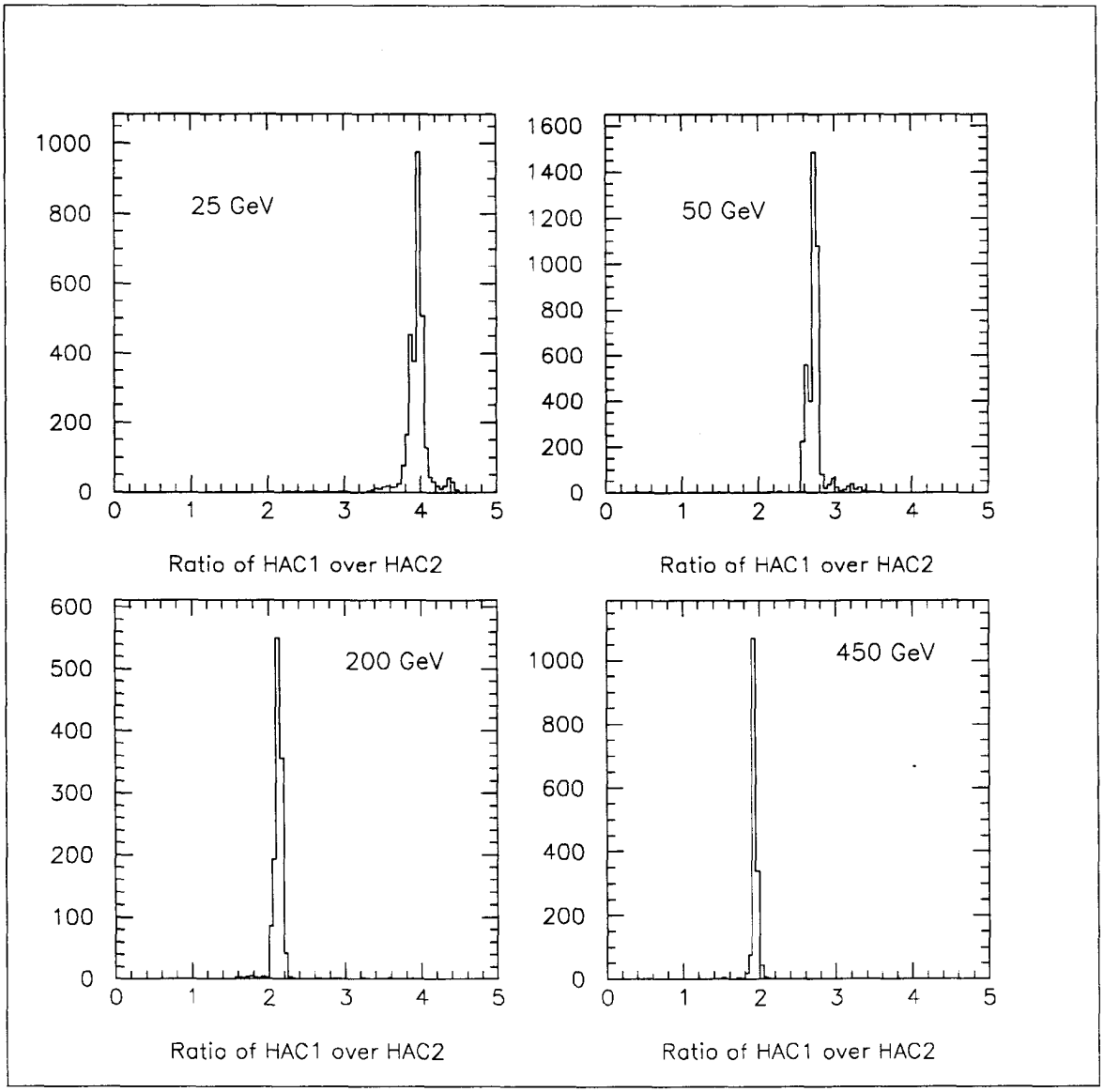

Figure 8: Ratio of energy in the first 5 layers (HAC1) to the energy in the next 4 layers (HAC2) at a) 25 GeV, b) 50 GeV, c) 200 GeV, and d) 450 GeV.

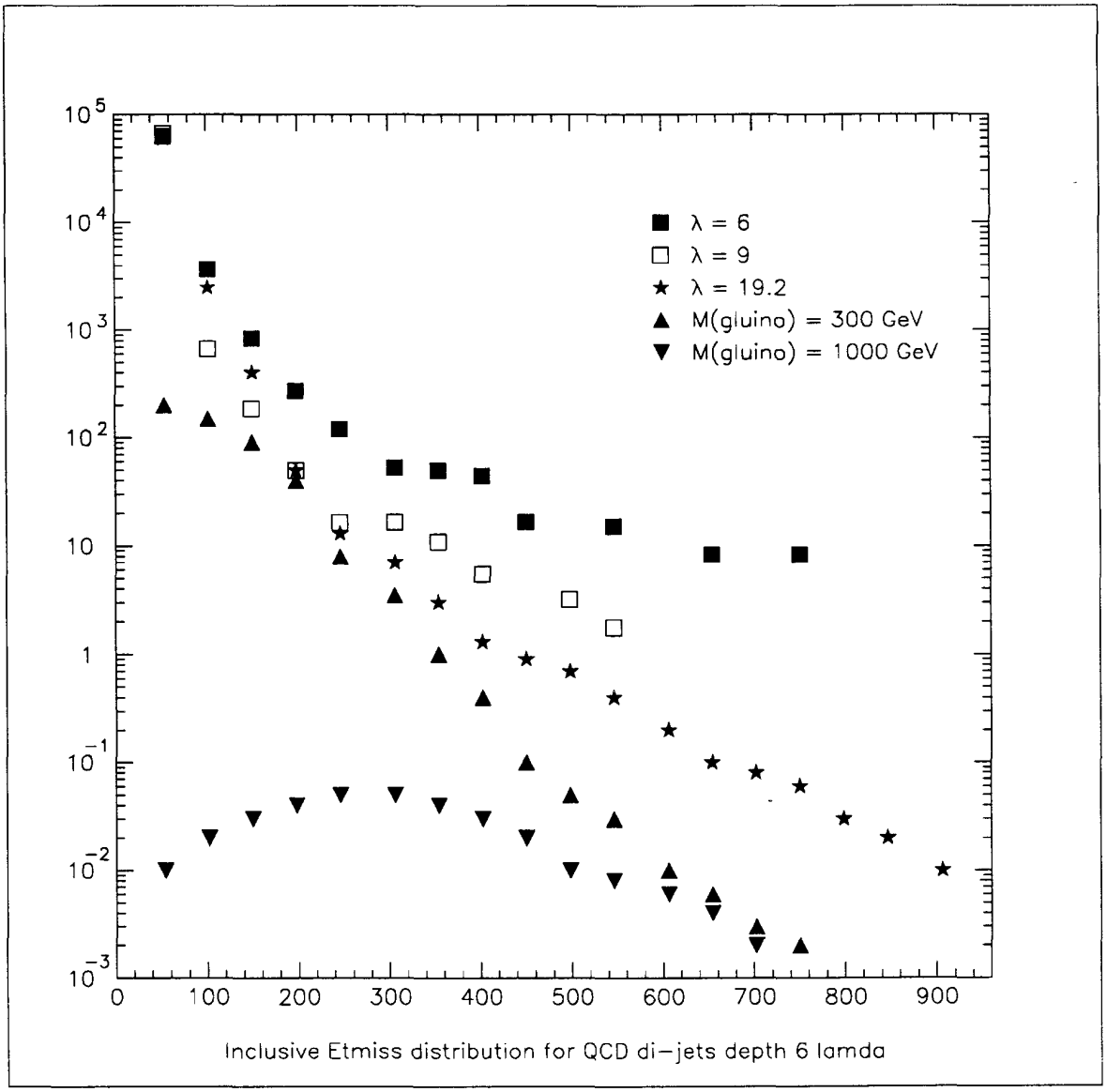

Figure 9: $d\sigma/d$(Missing E_T) (pb/ 50 GeV) for QCD dijet events. Also shown are the responses of a 6 λ and a 9 λ and an infinite 19.2 λ calorimeter. The level of rejection needed for new physics is also indicated by showing the signal expected for glinos of mass 300 and 1000 GeV.

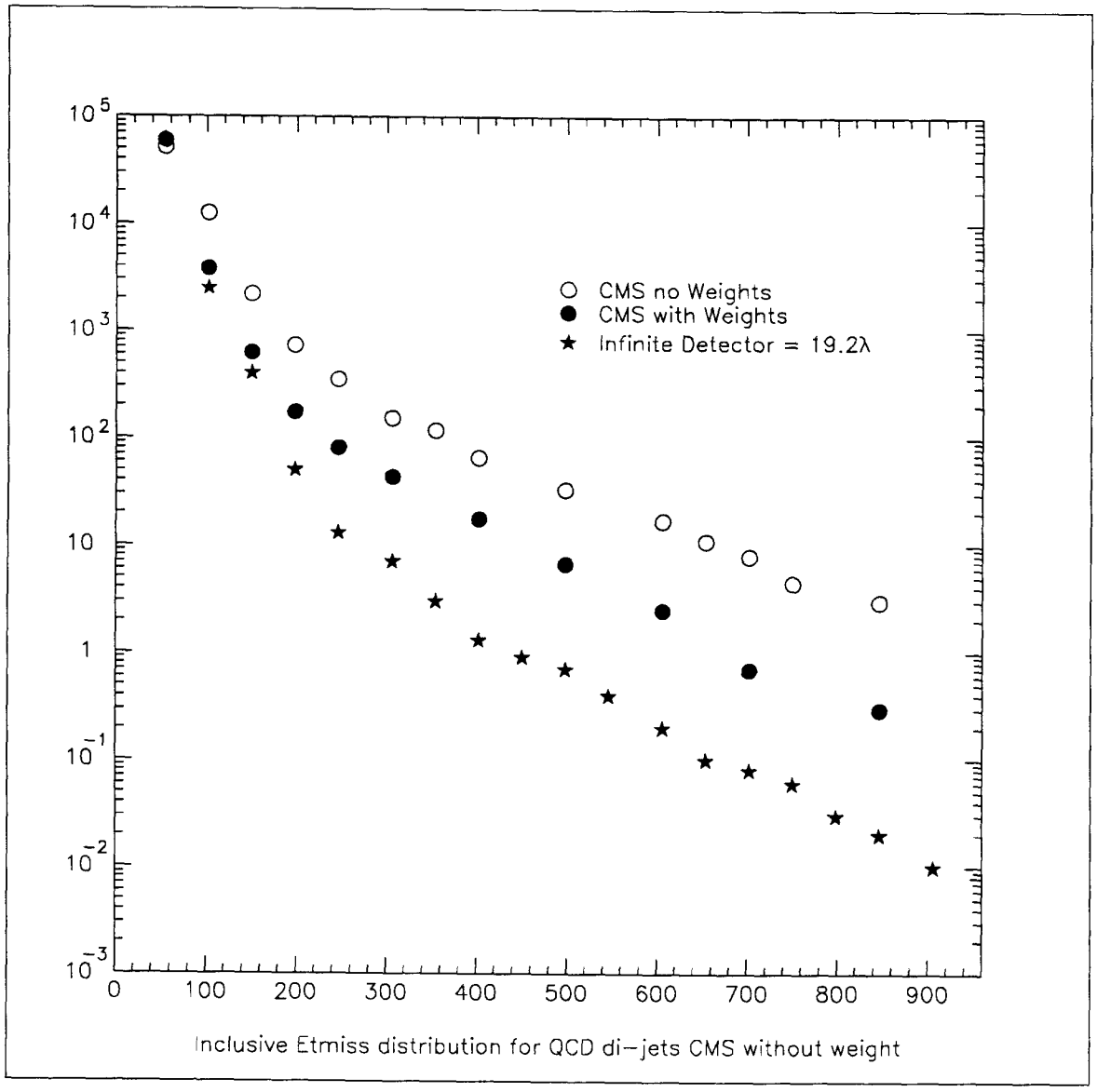

Figure 10: The missing E_T cross section for the CMS calorimeter for QCD dijet events. The vertical scale is $d\sigma/d(\text{Missing } E_T)$ (pb/ 50 GeV). The three sets of data points are for a standard an improved weighted, and an infinte (19.2 λ) calorimetr.